

Free form fabricated features on CoCr implants with and without hydroxyapatite coating *in vivo*: a comparative study of bone contact and bone growth induction

Kathryn Grandfield · Anders Palmquist · Stéphane Gonçalves · Andy Taylor · Mark Taylor · Lena Emanuelsson · Peter Thomsen · Håkan Engqvist

Received: 1 February 2010 / Accepted: 29 January 2011 / Published online: 9 February 2011
© Springer Science+Business Media, LLC 2011

Abstract The current study evaluates the *in vivo* response to free form fabricated cobalt chromium (CoCr) implants with and without hydroxyapatite (HA) plasma sprayed coatings. The free form fabrication method allowed for integration of complicated pyramidal surface structures on the cylindrical implant. Implants were press fit into the tibial metaphysis of nine New Zealand white rabbits. Animals were sacrificed and implants were removed and embedded. Histological analysis, histomorphometry and electron microscopy studies were performed. Focused ion beam was used to prepare thin sections for high-resolution transmission electron microscopy examination. The fabricated features allowed for effective bone in-growth and firm fixation after 6 weeks. Transmission electron microscopy investigations revealed

intimate bone-implant integration at the nanometre scale for the HA coated samples. In addition, histomorphometry revealed a significantly higher bone contact on HA coated implants compared to native CoCr implants. It is concluded that free form fabrication in combination with HA coating improves the early fixation in bone under experimental conditions.

1 Introduction

Implant fixation and interfacial stability remain important concerns for improving the longevity of orthopaedic prostheses. Incomplete anchorage at the implant–bone interface may lead to aseptic loosening and failed implantation [1]. Improved anchorage can be achieved by a number of approaches including cemented fixation, mechanical bone-implant interlocking, and bioactive fixation.

Cobalt chromium (CoCr) alloys have widespread use in the orthopaedics industry. Their mechanical properties qualify them as a suitable material for joint replacement including use in prosthetic hip femoral components and knee replacements [2, 3]. Cobalt chromium alloys have been used extensively as an alternative to titanium alloys due to their superior stiffness, corrosion resistance, and in particular, due to their greater surface hardness, which increases their resistance to wear *in vivo* [4]. Complete osseointegration depends on a number of factors including implant design and surface finish [5]. While conventional casting techniques constrain implant shape and design, the use of free form fabrication enables the production of advanced geometries to improve mechanical bone–metal interlocking at macroscopic surface features [6]. In this procedure, a focused laser beam is used for selective melting of the metal, enabling control of macro and micro

K. Grandfield (✉) · H. Engqvist
The Ångström Laboratory, Department of Engineering Sciences,
Uppsala University, Box 534, 751 21 Uppsala, Sweden
e-mail: kathryn.grandfield@angstrom.uu.se

A. Palmquist · L. Emanuelsson · P. Thomsen
Department of Biomaterials, Sahlgrenska Academy, University
of Gothenburg, Göteborg, Sweden

S. Gonçalves
Teknimed S.A, Vic en Bigorre, France

A. Taylor
Finsbury Development Limited, Leatherhead, UK

M. Taylor
Pera, Melton Mowbray, UK

P. Thomsen
Institute for Biomaterials and Cell Therapy (IBCT), Göteborg,
Sweden

dimensions of implants to facilitate bone in-growth. Previous studies have indicated that the controlled microstructure resulting from CAD–CAM produced CoCr implants results in improved bone growth compared to conventionally cast implants [6].

While the use of common cements such as PMMA may provide further implant anchorage, they are not without their disadvantages. The toxicity of the PMMA monomer, weak mechanical properties in tension, and thermal damage of tissue during polymerization are among the downfalls [5, 7]. Additionally, in cases of infection, the presence of cement can increase the difficulty of revision surgery [8]. Retrospective studies have shown good results for uncemented fixation compared to cemented [8, 9].

Hydroxyapatite (HA) coating is a standard method used in orthopaedics and dentistry to improve bioactive fixation of medical implants to bone [10, 11]. Due to the structural and chemical resemblance of HA to the inorganic constituent of bone, the coating is intended to enhance bone growth at the immediate implant–bone interface. Interface stability is achieved by means of bioactive fixation, ‘the interfacial bonding of an implant to tissue by formation of a biologically active HA layer on the implant surface’ [12]. This form of bioactive fixation provides an interface with strength equal to or greater than bone and removes the need for cemented fixation [12].

In this study, cylindrical CoCr implants with pyramidal surface structures were produced by free form fabrication. In addition to the fabrication of shape for effective bone intergrowth, the osseous response of plasma sprayed HA coatings was also evaluated. This paper presents the results from a comparative study between HA plasma sprayed and uncoated free form fabricated CoCr implants *in vivo* in a rabbit model.

2 Materials and methods

2.1 Implant and coating

Cylindrical shaped CoCr implants ($\phi = 4$ mm and $l = 5$ mm) were manufactured with pyramidal surface features using direct laser melting, a direct part manufacturing method (EOS, Germany). The technology fuses metal powder into the solid part by local melting using a focused laser beam. The final component is built up additively, layer-by-layer, directly from the 3D CAD models developed by Finsbury Development Limited. The laser sintered implants were characterized by a fine uniform crystal grain structure. The chemistry and properties of the CoCr implants meet the requirements of ISO 5832-4 and ASTM F75 for cast CoCrMo. In total nine implants were produced, and partially coated with HA. Hydroxyapatite

was prepared in an aqueous solution using the neutralisation method (Teknimed, Vic en Bigorre, France). A milk of lime solution was neutralised by the addition of a phosphoric acid solution, resulting in the production of large quantities of HA using little equipment. A standard plasma spraying scheme to coat the implants with HA was employed. Plasma spraying was carried out using a 2PS atmospheric plasma spray installation (Projection Plasma Système, France) including a GT5 torch with external powder injector and 2PS powder feeder. Argon and hydrogen were used at constant flow rate to produce the plasma. The HA powder feed rate, controlled by a vibrating system, was kept constant. Argon was used as the carrier gas. Thickness and repartition of the coating were controlled by 5-axis CNC equipment. The coating procedure involved masking half of the sample, cleaning the exposed side, followed by introducing the HA powder into the plasma jet stream, where it was heated and subsequently deposited onto the metal implant surface. The coating thickness varied along the pyramidal features from 112 ± 8 μm at the top, 169 ± 18 μm at the bottom, to 71 ± 3 μm on the sides of the pyramids. An example of an uncoated and coated implant is seen in Fig. 1a. Due to the small sample size and geometries it was difficult to obtain an even coating over the surface structures. Consequently, the peaks of the pyramids and the outer surface of the cylinder received a thicker coating.

2.2 Cleaning and sterilization

After coating, all implants were subjected to ultrasound cleaning in ethanol (70%) for 1 min. Implants were then placed in glass tubes with plastic cover lids followed by gamma sterilization (25 Gy) (Sterigenics, Copenhagen, Denmark).

2.3 Animals and surgical procedures

Nine female adult New Zealand white rabbits, with weights ranging between 4 and 6 kg (mean 5 kg), were used for *in vivo* evaluation. Animals were fed ad libitum and prior to surgery anaesthetized by intramuscular (i.m.) injections of fluanizone (Hypnorm[®], Janssen, Brussels, Belgium; 0.7 mg/kg b.wt. (body weight)) and intraperitoneal (i.p.) injection of diazepam (Stesolid[®], Dumex, Copenhagen, Denmark; 1.5 mg/kg b.wt.). The implants were inserted in the tibial metaphysis where a hole was drilled using a dental guide drill at low speed, 2,500 rounds per minute, using generous irrigation with cold saline. The implants were press fit into the holes with the upper surface level at the cortical bone surface, see Fig. 1b. After insertion the operation site was rinsed with saline and sutured in separate layers with

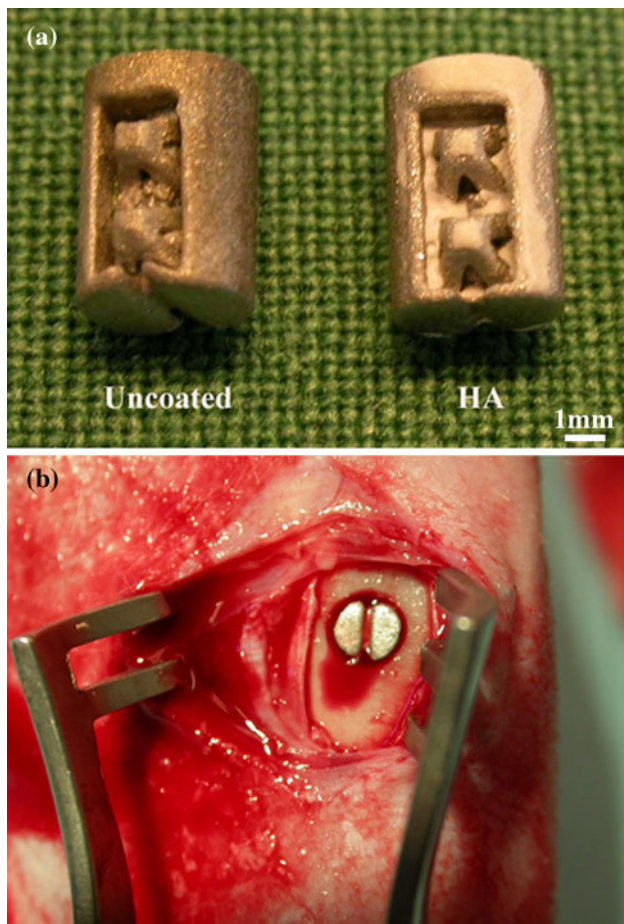


Fig. 1 **a** Photograph of the free form fabricated uncoated and coated CoCr implants, showing the pyramidal surface features. **b** Photograph of the implant site

Vicryl® 5-0 and finally with intracutaneus Monocryl® 4-0. Surgery time was about 1 h per animal.

Prior to surgery and 2 days postoperatively, animals were given sulfadoxin/trimethoprim (Borgal® vet 0.5 ml/kg b.wt/day). Three days postoperatively the animals received analgesics (Bupenorphine®, Temgesic, Reckitt and Colman, USA, 0.05 mg/kg b.wt/day) as i.m. injections. Initially, all animals were housed separately but after 1 week housed together to allow a greater range of freedom.

For fluorescence detection at different stages of the bone growth process Oxytetracycline (Sigma, St. Louis, USA; 25 mg/kg b.wt i.m.) and Alizarin Complexone (Sigma, St. Louis, USA; 50 mg/kg b.wt i.m.) were injected subcutaneously 2 and 1 week before sacrifice, respectively.

The Animal Ethical Committee at University of Gothenburg provided ethical consent for the study.

2.4 Retrieval and specimen processing

Animals were sacrificed after 6 weeks by an intra-venous overdose of pentobarbital (Mebumal®, ACO Läkemedel

AB, Solna, Sweden). Tissue fixation was performed by perfusion with 2.5% gluteraldehyde in 50 mM sodium cacodylate buffer (pH 7.4) injected into the animals via the left heart ventricle. The implants and the surrounding tissue were removed *en bloc* followed by further fixation by immersion in gluteraldehyde for 3 days and postfixed in 1% osmium tetroxide for 2 h. Samples were stepwise dried with immersion in increasing concentrations of ethanol (95–100%), and thereafter embedded in plastic resin (LR White, The London Resin Co Ltd, Hampshire, UK). The blocks were divided through the long axis of each implant using a band saw (Exakt cutting and grinding equipment, Exakt Apparatebau, Norderstedt, Germany). Ground sections were prepared for fluoroscopy (40 µm, unstained) and morphometry (15 µm, stained with 1% toluidine blue) [13]. An FEI Strata DB325 dual beam focused ion beam (FIB) equipped with an Omniprobe lift-out system was used for production of electron transparent TEM samples (thickness < 100 nm) from blocks. The dual beam SEM/FIB system allowed for site-specific selection of interface regions in SEM mode, and subsequent milling of material using a 30 kV gallium ion source. Thin lamellae produced were lifted out and attached to TEM grids using an *in situ* lift-out method [14].

2.5 Analysis

An E600 Nikon Eclipse light microscope was used for qualitative histological evaluation. An example of a ground-section used for the evaluation is shown in Fig. 2. The morphometric measurements included (i) calculation of the degree of bone-implant contact, expressed as mean percentage bone contact along the implant surface and

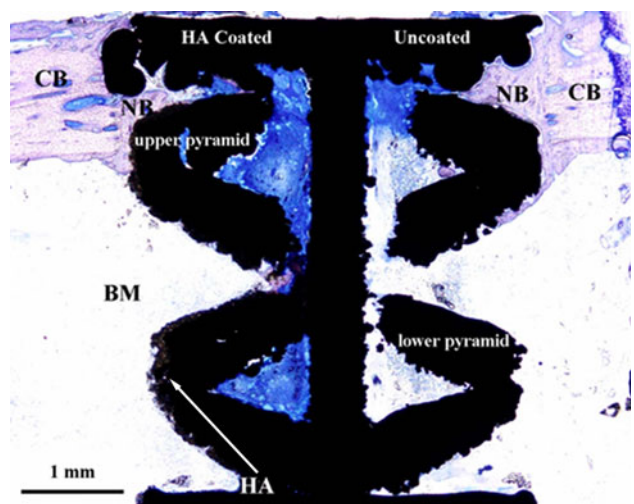


Fig. 2 Light microscopy. The implant cut along the long axis, showing new bone growth (NB) into both HA coated and uncoated sides. BM bone marrow, CB cortical bone

(ii) amount of bone within the valleys around the fabricated pyramids, expressed as mean percentage bone area.

Ultrastructural analysis of the bone–HA interface was done using an FEI Tecnai F30 ST TEM equipped with a Gatan Imaging Filter and operated at 300 kV. Samples were analyzed from a cryo sample holder with liquid nitrogen cooling, to avoid electron beam damage to the bone tissue.

2.6 Statistics

Histomorphometry data was evaluated using the Wilcoxon sign rank test (SPSS 13.0, SPSS Inc., Chicago, USA).

3 Results

3.1 Qualitative evaluation

All surgical sites healed uneventful. Ground sections prepared for light microscopy and fluoroscopy were used for histology. A general observation from the prepared samples was newly formed bone growth into the pyramids of the macrostructure (Fig. 2). At the time of retrieval, 6 weeks after implantation, bone had grown in contact with a major part of the implant surface at the level of the cortical bone. Islands of soft tissue were occasionally observed intervening between bone and the uncoated CoCr surface (Fig. 3). This was not seen for the coated site, indicating a larger degree of bone contact for HA coated implants.

Fluoroscopy demonstrated an on-going bone formation process leading to densification near the implant surface. Oxytetracycline fluorostate, injected in the animals 2 weeks prior to sacrificing, showed new bone growth at the metal coating surface (Fig. 4a). When the fluoroscope was set to highlight Alizarin, injected 1 week prior to retrieval, islands of continued bone growth were detected (Fig. 4b). No intervening fibrous capsule or inflammation can be seen. The adhesion of the coating was sufficient in that it did not delaminate during implantation; neither remnants of the ceramic coating nor metal particles were detected in the surrounding tissue.

3.2 Quantitative evaluation

Histomorphometric analysis showed a significant ($P < 0.05$) increase in bone contact measured along the length of the implant surface on HA coated samples (Fig. 5). New bone grew on $26 \pm 6\%$ of the implant surface of the coated side of implants, compared to only $11 \pm 2\%$ bone growth on the native CoCr surface.

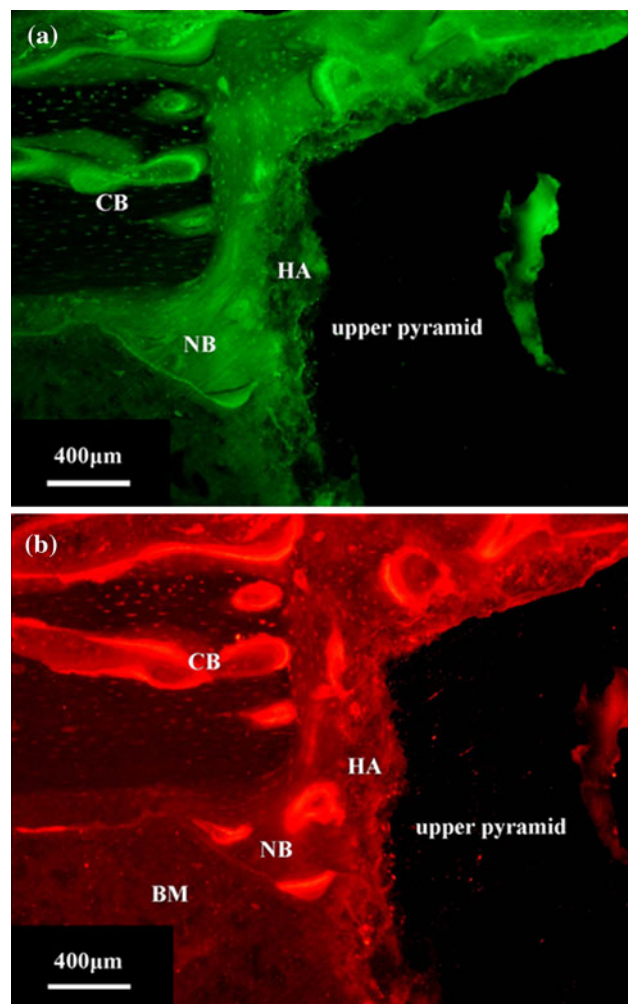


Fig. 3 Fluoroscopy. **a** Oxytetracycline labelling. New bone growth at the interface and ongoing remodelling of the bone tissue are seen. **b** Alizarine labelling. Further growth in islands in the new and old bone leading to densification is seen. *CB* cortical bone, *NB* new bone, *BM* bone marrow and *HA* hydroxyapatite coating

Quantification of bone area around the implants, within the valleys around the fabricated pyramidal features, gave no significant observed difference ($P < 0.02$) (Fig. 6).

3.3 Ultrastructural analysis

Samples for transmission electron microscopy (TEM) of the bone–implant interface were produced using a FIB *in situ* lift-out method shown in Fig. 7. TEM revealed an intimate interaction at the HA–bone interface (Fig. 8a). The dark field electron micrograph, recorded from the interface in Fig. 8b, shows a jagged outermost part of the coating. This observation is indicative of resorption of the HA coating in the bone. Sample preparation of an intact CoCr–bone interface was not possible. All produced sample slices had a gap between the CoCr metal and bone.

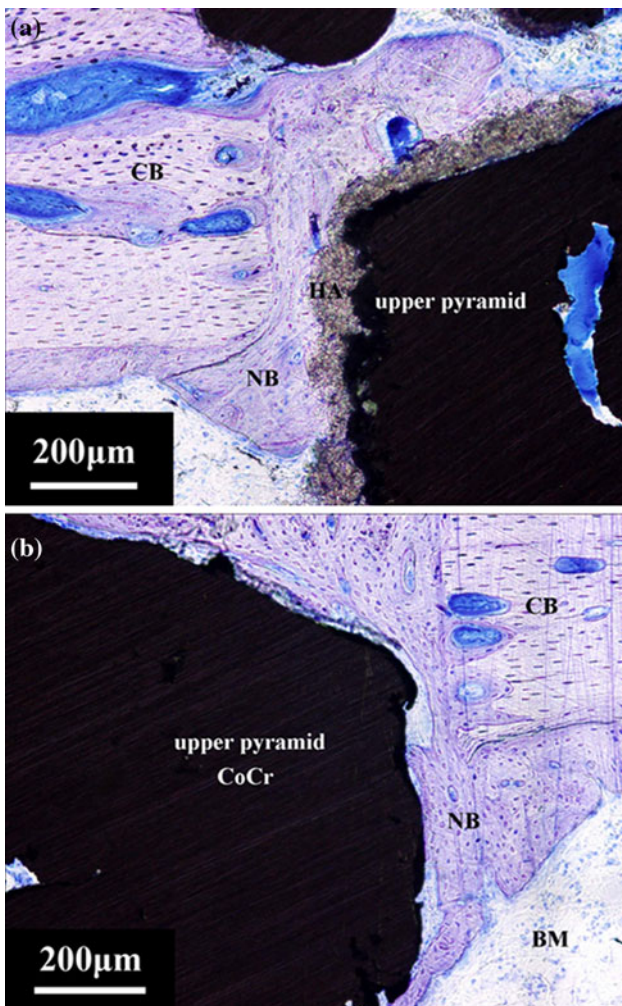


Fig. 4 High magnification light microscopy images of the coated (a) and the uncoated (b) side of the implant. Soft tissue is seen at the interface region of the uncoated side

Bone shrinkage during retrieval and weak adhesion at the interface will lead to separation of the materials. When cracks were found in the HA-bone samples (Fig. 8c), separation was found in the bone rather than at the interface. Thus indicating that the higher strength of the HA-bone interface involves chemical bonding.

4 Discussion

Free form fabrication provides an effective method to produce complex implant geometries in a reproducible manner, where both surface structures and interconnected pores within the implant could be produced in different materials [15, 16]. In the present study, pyramidal surface features on cylindrical CoCr implants were evaluated. Such features, important to improve mechanical bone-metal interlocking, are otherwise difficult to achieve with

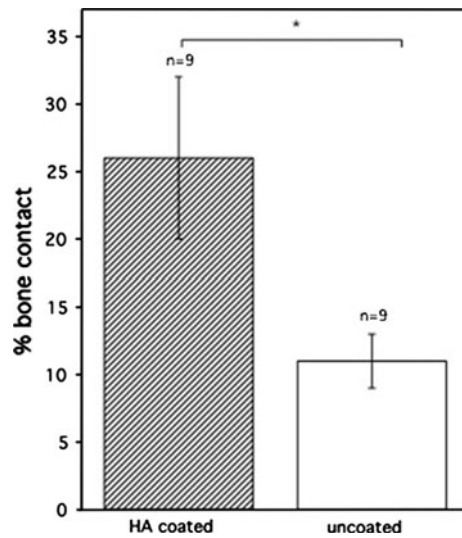


Fig. 5 Histogram of bone-implant contact for HA coated and uncoated surfaces. A significant difference ($P < 0.05$) between the surfaces is indicated by asterisk

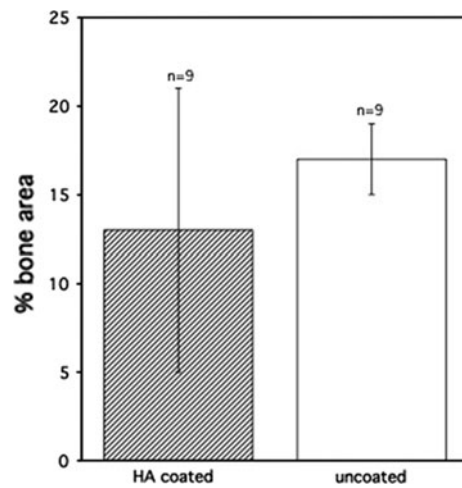


Fig. 6 Histogram presenting measured bone area within the fabricated features. No statistically significant difference ($P < 0.02$) could be observed comparing the coated with the uncoated side

conventional casting [6]. The ability to produce finely controlled macro-topographies on CoCr alloys has been demonstrated with 3D printing method [17]. In addition, the macro 3D-printed features on CoCr implants have been shown to significantly improve bone in-growth in vivo compared to non-patterned surfaces [18]. The histomorphometry revealed a high degree of bone growth into the fabricated features after 6 weeks implantation of both coated and uncoated implants. Qualitative evaluation of ground sections revealed newly formed bone between the original compact bone and implant surface, as well as bone in-growth in the hollow compartment around the pyramids.

Fig. 7 Focused ion beam preparation method of thin section for TEM analysis outlined sequentially in images (a–d)

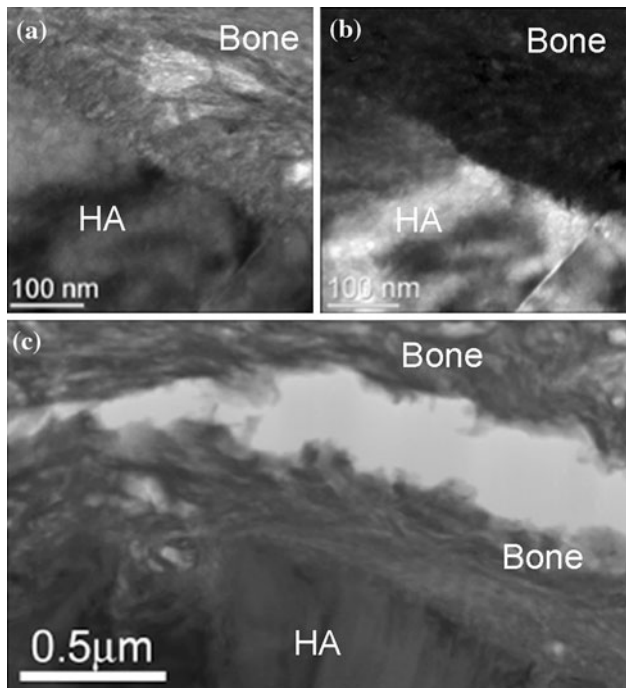
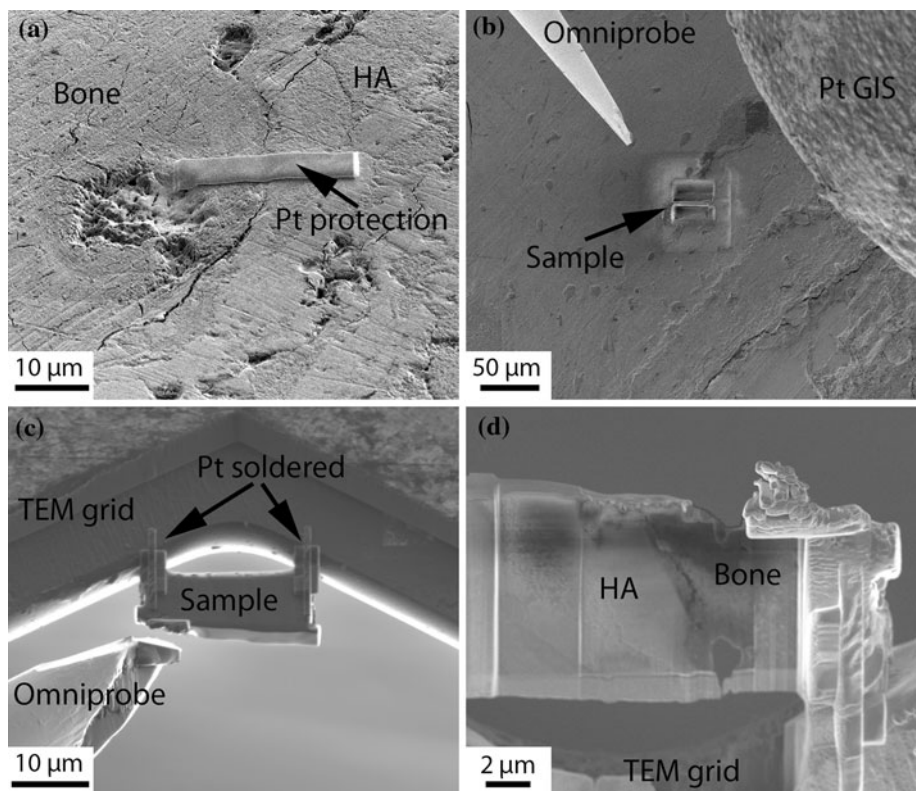


Fig. 8 TEM images of the hydroxyapatite–bone interface. Bright field (a) and dark field (b) images indicating bone growth directly at the outermost surface and resorption of the synthetic hydroxyapatite. Low magnification TEM image (c) shows a crack in the bone rather than at the interface, indicating a strong adhesion at the HA–bone interface

In addition, fluoroscopy revealed active remodelling of bone surrounding the implant during the test period.

Applying a plasma sprayed coating of HA to implants significantly improved in vivo interaction. Although bone area measurements did not indicate improved performance of coated versus uncoated implants, bone contact measurements exhibited a significant increase. This phenomena has been reported earlier, where a significant increase in bone–implant contact was achieved with HA coatings while the bone area around the implant was similar or even decreased for the coated specimens [19, 20]. Further, it has also been observed for rough versus smooth titanium implants, where both the bone–implant contact and the removal torque was significantly increased for rougher surfaces while the bone area around the implants were higher for the smoother surface [21]. Previous studies have demonstrated significant correlations between torque and the percentage of bone in contact with the implant, and between pull-out load and the bone thickness around the implant [22]. Whether the increased fixation is related to bone bonding or mechanical interlocking is unknown. By using novel techniques for ultrastructural evaluations of the bone–implant interface a more thorough understanding of the bonding mechanisms could be achieved [23].

Evidence of improved anchorage was also demonstrated by the HA–bone interface analyzed by TEM. Preparation of a native CoCr–bone interface sample was not possible

since implant-bone separation was noted in all attempts. It is unclear if separation was due to retrieval artifacts or lack of sufficient bone contact. For the HA coating, a jagged interface was observed in the TEM due to dissolution of the HA coating in the bone tissue. This has been shown for sintered carbonate and silicon substituted HA in bone, especially occurring at the triple junction of the sintered grains [24, 25]. It was also suggested that the dissolution was more intense with substituted ions compared to pure HA. No dissolution was observed with sintered nano-porous scaffolds [26]. However, the difference in crystal structure and crystallinity of the plasma sprayed coatings compared to sintered scaffolds most likely changes the solubility. Further, the HA coated sample revealed cracking in the bone material rather than at the HA–bone interface, indicating bioactive fixation and an interface with higher strength than the bone tissue [12].

The incorporation of an HA coating may lead to other advantages. The release of metallic ions such as Co and Cr at the implant surface may induce periprosthetic bone loss, leading to aseptic loosening and implant failure [27]. The addition of a biocompatible layer, such as HA, may act as a buffer to prevent the release of biologically harmful metallic ions.

5 Summary and conclusion

Cobalt chromium implants with designed surface features were produced using free form fabrication. Half of each implant was coated with HA and press fit into the limbs of nine New Zealand white rabbits. The present studies demonstrated a significantly larger level of bone contact on HA coated implants compared to the native CoCr surface. TEM revealed intimate bone-implant integration at the nanometre scale for the HA coated samples and evidence of resorption and increased interface strength. Taken together, the results suggest free form fabrication is a versatile production method to achieve complex surface structures. Further, the interfacial biological response to such surface structures could be enhanced by HA coating.

Acknowledgments European Commission Project Hiped Hips 2 (Proposal number CRAFT – 1999 – 70587), VINNOVA VinnVäxt Program Biomedical Development in Western Sweden, the Swedish Research Council (grant K2006-73X-09495-16-3), the Institute of Biomaterials and Cell Therapy (IBCT), the Göran Gustafsson Foundation, and Teknimed are gratefully acknowledged.

References

- Sundfeldt M, Carlsson LV, Johansson CB, Thomsen P, Gretzer C. Aseptic loosening, not only a question of wear: a review of different theories. *Acta Orthop.* 2006;77(2):177–97.
- Webster TJ, Ejiofor JU. Increased osteoblast adhesion on nanophasic metals: Ti, Ti6Al4V and CoCrMo. *Biomaterials.* 2004;25:4731–9.
- Rahaman MN, Yao A, Bal BS, Garino JP, Ries MD. Ceramics for prosthetic hip and knee joint replacement. *J Am Ceram Soc.* 2007;90(7):1965–88.
- Sotereanos NG, Engh CA, Glassman AH, Marcalino GE, Engh CA Jr. Cementless femoral component should be made from cobalt chrome. *Clin Orthop Relat Res.* 1995;313:146–53.
- Walsh WR, Svehla MJ, Russell J, Saito M, Nakashima T, Gillies RM, Bruce W, Hori R. Cemented fixation with PMMA or Bis-GMA resin hydroxyapatite cement: effect of implant surface roughness. *Biomaterials.* 2004;25:4929–34.
- Hunt JA, Callaghan JT, Sutcliffe CJ, Morgan RH, Halford B, Black RA. The design and production of Co-Cr alloy implants with controlled surface topography by CAD/CAM method and their effects on osseointegration. *Biomaterials.* 2005;26(29):5890–7.
- Villar RN. Non-cemented hip prosthesis. *Br Med J (Clin Res Ed).* 1985;291:53.
- Gao F, Henricson A, Nilsson KG. Cemented versus uncemented fixation of the femoral component of the NexGen CR total knee replacement in patients younger than 60 years: a prospective randomised controlled RSA study. *Knee.* 2009;16:200–6.
- Bojescul JA, Xenos JS, Callaghan JJ, Savory CG. Results of porous-coated anatomic total hip arthroplasty without cement at fifteen years: a concise follow-up of a previous report. *J Bone Joint Surg Am.* 2003;85:1079–83.
- Ong JL, Chan DCN. Hydroxyapatite and their use as coatings in dental implants: a review. *Crit Rev Biomed Eng.* 2000;28(5–6):667A–707A.
- Chambers B, St. Clair SF, Froimson MI. Hydroxyapatite-coated tapered cementless femoral components in total hip arthroplasty. *J Arthroplast.* 2007;22(4):71–4.
- Hench LL. Biomaterials: a forecast for the future. *Biomaterials.* 1998;19(16):1419–23.
- Donath K, Breuner G. A method for the study of decalcified bones and teeth with attached soft tissues. The Sage-Schiff(sawing and grinding) technique. *J Oral Pathol.* 1982;11:318–26.
- Jarmar T, Palmquist A, Bränemark R, Hermansson L, Engqvist H, Thomsen P. Technique for preparation and characterization in cross-section of oral titanium implant surfaces using focused ion beam and transmission electron microscopy. *J Biomed Mater Res.* 2008;87A:1003–9.
- Malmström J, Adolfsson E, Emanuelsson L, Thomsen P. Bone ingrowth in zirconia and hydroxyapatite scaffolds with identical macroporosity. *J Mater Sci Mater Med.* 2008;19:2983–92.
- Thomsen P, Malmström J, Emanuelsson L, René M, Snis A. Electron beam-melted, free-form-fabricated titanium alloy implants: material surface characterization and early bone response in rabbits. *J Biomed Mater Res.* 2009;90B:35–44.
- Curodeau A, Sachs E, Caldarise S. Design and fabrication of cast orthopedic implants with freeform surface textures from 3-D printed ceramic shell. *J Biomed Mater Res.* 2000;53:525–35.
- Melican MC, Zimmerman MC, Dhillon MS, Ponnambalam AR, Curodeau A, Parsons JR. Three-dimensional printing and porous metallic surfaces: a new orthopedic application. *J Biomed Mater Res.* 2001;55:194–202.
- Mohammadi S, Esposito M, Hall J, Emanuelsson L, Krozer A, Thomsen P. Long-term bone response to titanium implants coated with thin radiofrequency magnetron sputtered hydroxyapatite in rabbits. *Int J Oral Maxillofac Implants.* 2004;19:498–509.
- Wennerberg A, Hallgren C, Johansson C, Danelli S. A histomorphometric evaluation of screw-shaped implants each prepared with two surface roughnesses. *Clin Oral Implants Res.* 1998;9:11–9.

21. Wennerberg A, Albrektsson T, Andersson B, Krol JJ. A histomorphometric and removal torque study of screw-shaped titanium implants with three different surface topographies. *Clin Oral Implants Res.* 1995;6:24–30.
22. Bränemark R, Ohrnell LO, Nilsson P, Thomsen P. Biomechanical characterization of osseointegration during healing: an experimental in vivo study in the rat. *Biomaterials.* 1997;18(14): 969–78.
23. Engqvist H, Botton GA, Couillard M, Mohammadi S, Malmström J, Emanuelsson L, Hermansson L, Phaneuf MW, Thomsen P. A novel tool for high-resolution transmission electron microscopy of intact interfaces between bone and metallic implants. *J Biomed Mater Res.* 2006;78A:20–4.
24. Porter A, Patel N, Brooks R, Best S, Rushton N, Bonfield W. Effect of carbonate substitution on the ultrastructural characteristics of hydroxyapatite implants. *J Mater Sci Mater Med.* 2005; 16(10):899–907.
25. Porter AE, Buckland T, Hing K, Best SM, Bonfield W. The structure of the bond between bone and porous silicon-substituted hydroxyapatite bioceramic implants. *J Biomed Mater Res.* 2006; 78A:25–33.
26. Malmström J, Slotte C, Adolfsson E, Norderyd O, Thomsen P. Bone response to free form-fabricated hydroxyapatite and zirconia scaffolds: a histological study in the human maxilla. *Clin Oral Implants Res.* 2009;20:379–85.
27. Haynes DR, Crotti T, Haywood MR. Corrosion of and changes in biological effects of cobalt chrome alloy and 316L stainless steel prosthetic particles with age. *J Biomed Mater Res.* 2000;49: 167–75.